Received: 26 April 2021 | Revised: 3 June 2021 | Accepted: 7 June 2021

DOI: 10.1002/ppap.202100062

RESEARCH ARTICLE

PLASMA PROCESSES AND POLYMERS

Validation of colorimetric assays for hydrogen peroxide, nitrate and nitrite ions in complex plasma-treated water solutions

Valeria Veronico[1] | **Pietro Favia**[1,2] | **Francesco Fracassi**[1,2] | **Roberto Gristina**[2] | **Eloisa Sardella**[2]

[1]Department of Chemistry, University of Bari Aldo Moro, Bari, Italy

[2]CNR–Institute of Nanotechnology (CNR-NANOTEC) UoS Bari c/o Department of Chemistry, University of Bari Aldo Moro, Bari, Italy

Correspondence
Eloisa Sardella,CNR–Institute of Nanotechnology (CNR-NANOTEC) UoS Bari c/o Department of Chemistry.
Email: eloisa.sardella@cnr.it

Funding information
Laboratorio Pubblico di ricerca Industriale e Pugliese dei Plasmi, within the Framework Programme Agreement APQ "Ricerca Scientifica", II atto integrative-Reti di Laboratori Pubblici di Ricerca, Grant/Award Number: 51; intra-Institute project CNR-NANOTEC SEED.

Abstract

Liquids treated with cold plasma emerged as 'redox drugs' in biomedicine, as sources of reactive oxygen and nitrogen species targeting cellular functions, including wound healing and cancer progression. The use of cell culture media as starting liquid, however, challenges the identification of plasma-generated chemistry, limited by the presence of many reactive species and organic compounds. Available detection methods need, therefore, to be confirmed in these liquids to avoid inaccurate results. In this research, robustness, linearity, accuracy and specificity of three colorimetric assays are investigated to detect H_2O_2, NO_2^- and NO_3^-, predominant plasma-induced products. The results clearly highlight the presence of some factors affecting the detection in cell culture media like high concentrations of chlorides found interfering with the detection of NO_3^- in the medium.

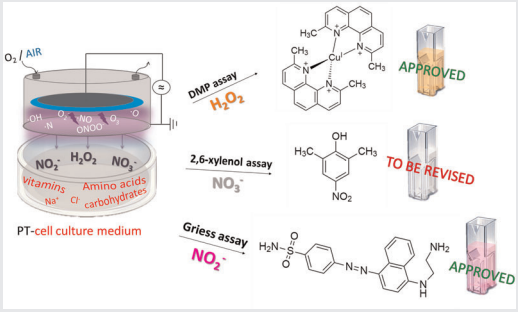

KEYWORDS
colorimetric reactions, plasma-treated water solutions, reactive oxygen and nitrogen species, spectroscopic methods

Abbreviations: AP-NTP, atmospheric pressure nonthermal plasmas; DBD, dielectric barrier discharge; DMEM, Dulbecco's Modified Eagle's Medium; PT, plasma-treated; PTWS, plasma-treated water solutions; RONS, reactive oxygen and nitrogen species.

1 | INTRODUCTION

Nonthermal plasmas (NTP) are, by definition, ionised gases far from thermodynamic equilibrium, whose processes, applications and products are in continuous growth in several scientific and technological fields.[1,2] Surface modification processes for biomaterials have been the most popular outcomes of NTP in the biomedical area for about 50 years.[1,3] In the last one-two decades, though, NTP are being continuously proposed for newer uses in Life Sciences, namely, for the decontamination of wounds,[4] for cancer treatments,[5,6] and for activating water and seeds to improve germination and harvest.[7] The NTP processes investigated in this direction are ignited at atmospheric pressure (AP), generally in air or other gases including inert ones, in close proximity to living matter or water-based liquids. Direct NTP treatments of cells and tissues, as well as the synthesis of plasma-treated water solutions (PTWS), namely aqueous media enriched with reactive oxygen and nitrogen species (RONS) upon exposure to NTP, recently gained attention as novel promising treatments capable to target specific redox-controlled biological pathways for therapeutic purposes.[8]

PTWS can be easily generated through the exposure of liquids to atmospheric pressure nonthermal plasmas (AP-NTP), namely to electrons, ions, radicals and neutral atomic/molecular fragments in different states, in presence of electric field and UV photons. When O_2 and N_2 mixtures are used to feed the processes, gaseous blends of (primary) RONS are generated in the plasma,[9] which can dissolve in the treated liquid. Cross reactions of primary RONS among them or with other components in the liquid generally extinguish transient reactive RONS in favour of most stable (secondary) RONS, such as hydrogen peroxide (H_2O_2), nitrate (NO_3^-) and nitrite (NO_2^-) ions, usually found in PTWS.[10]

Thanks to the possibility to control the chemical composition of the plasma and to treat any liquid, including those used in biology and medicine,[11] PTWS are widely tuneable RONS-releasing vectors available for biomedical applications, from stimulation of wound healing,[4] to pathogen decontamination/sterilisation,[12,13] till cancer treatment.[14–16] In these applications, PTWS are often produced by AP-NTP treatment of cell culture media (i.e., complex liquid media containing carbohydrates, vitamins, growth factors, amino acids and inorganic salts) that can further be used for biological experiments.[17–21] Even though promising results attested the clinical efficacy of PTWS, however, it quickly emerged that a careful control of the dose and the type of the RONS generated is a fundamental requirement to balance beneficial and deleterious effects of PTWS on malignant and healthy cells.[22,23]

The main limitation to achieve a fine dose control of RONS is currently due to their complicated detection in matrices like PTWS, challenged by potential inaccuracies and artefacts.[24] PTWS usually contain many RONS at the same time, which also react among each other and with components of the liquid. These reactions could also persist after the plasma treatment, leading to ageing processes that are still the object of investigation.[25] Most transient RONS generally recombine and react once diffused from the plasma into the liquid, but they can also be formed again from cross reactions among stable RONS, above all when in contact with cells.[23,26] As these reactions occur in the liquid, its chemical composition, altered with the plasma exposure, is decisive in this contest. To the complex panorama of chemical reactions in the plasma phase, in fact, it must be added the complexity of synergistic plasma-liquid chemistry, which is not simply the transfer of gas-phase species to the exposed liquids. The aftermath of such balance between RONS diffusion and reactivity in the liquid is a dynamic and complicated chemical composition that can dramatically change depending on the liquid treated. In the case of non-buffered liquids, for example, exposure to plasma is known to cause the acidification of the treated solution, further complicating the detection.[27] In the many different cell culture media available, RONS cross reactions occur in presence of usually more than 30 compounds in high concentrations among amino acids, vitamins, carbohydrates and inorganic salts. Massive differences among different cell culture media deal, for example, with the concentration of antioxidants species,[26] which are clearly involved, by definition, in the scavenging of oxidant species, including plasma-generated RONS. As a result, the RONS enrichment of each medium can significantly vary from one liquid to another, along with the oxidation of organic molecules present in the medium.[28,29]

The complex chemical composition in PT-cell culture media increases very much the difficulty of unambiguously identifying the RONS possibly responsible for effects on cells or tissues. In addition, the lack of absolute standardisation of commercial and home-made plasma sources, along with the operational conditions, makes it hard also to standardise the treatments used to generate PTWS.[26] Correspondingly, in absence of accurate chemical characterisation of the liquid composition, there is hardly a way to compare results obtained with PT-cell culture media for fully understanding the mechanisms at the base of their biological efficacy.

In our previous works we observed that the selective anticancer effects of PT-Dulbecco's Modified Eagle's

Medium (DMEM) on osteosarcoma cancer cells, with respect to endothelial ones, were strongly related to precise proportions between the concentration of H_2O_2 and NO_2^- ions in the treated media with a synergistic effect.[30]

It is, therefore, quite clear that the correct identification of the bioactive chemistry of these liquids should run in parallel with the availability of robust analytical techniques able to grant accurate and fast results even in such complex environments. So far, this correspondence is not fully reached and part of Plasma Medicine research is currently focused on the improvement of detection techniques currently available for RONS to avoid artefacts.

Selectivity is one of the main concerns, for example, due to the simultaneous presence of many RONS in PTWS originated in cell culture and other media.[24] The high concentrations of inorganic ions to grant cyto-compatible isotonic conditions and of many organic compounds in cell culture media, make inapplicable powerful techniques such as ion chromatography, electrochemical analysis or mass spectrometry, where the discrimination of signals generated from single molecules would be very complex. Moreover, the wide compositional range of PTWS impairs the possibility to standardise and optimise an univocal protocol of analysis to be extended to the detection of RONS in all possible environments.

Many efforts have been, therefore, spent in developing, adapting and optimising analytical methods to the complexity of such liquids. The list of the methods available for measurement of RONS in liquids has been reviewed by Bruggeman et al.,[31] whereas Khlyustova et al.[32] more specifically listed those used up to now in Plasma Medicine. Direct measurement of RONS in PTWS is achieved in water or simple water solutions (i.e., phosphate buffer, NaCl) by means of electrochemical,[33] chromatographic[34] or UV absorption methods.[35–37] The most common approach, however, is the indirect detection through the use of chemicals sensitive to specific RONS, such as spin traps,[38–41] fluorimetric,[42,43] chemiluminescent,[44] electrochemical[45] and colorimetric probes.[17,46–48] In consideration of ease and high robustness towards drastic variations in the environment in which they are performed, colorimetric and fluorimetric assays are widely established as the most common method to detect H_2O_2, NO_2^- and NO_3^-.[17,47,48] A multitude of colorimetric reactions are known to date. Table 1 summarises the most popular assays for the colorimetric/fluorimetric detection of H_2O_2, NO_2^- and NO_3^-, along with the well-known detection drawbacks in different liquids.

Concerning H_2O_2, most commercially available assays are based on oxidation reactions between a sensitive probe and H_2O_2. These reactions generally are not specific, so many oxidants could compete; thus, the main drawback reported for colorimetric detection of H_2O_2 in PTWS (i.e., Amplex Red®, titanyl sulphate assays and others) is the poor specificity. In spite of this, the Amplex Red®[40,57,58] method remains the most popular probe to detect H_2O_2 in PTWS generated from water, PBS and cell culture media, even if its specificity is challenged by peroxynitrite $ONOO^-$ anions, possibly present in those PT liquids.[59]

A method quite unexplored to detect H_2O_2 in PTWS is the colorimetric copper-phenanthroline assay, where H_2O_2, in presence of the phenanthroline derivative 2,9-dimethyl-1,10-phenanthroline (DMP), reduces copper(II) ions to a yellow–orange copper(I) complex with DMP, which is determined photometrically.[67–71] An important advantage of this assay for PTWS is that it is based on H_2O_2 behaving as a reducer rather than an oxidant,[72] in a system where the oxidant species usually formed can interfere. DMP is a commercially available reagent, soluble in water and the assay is a rapid one-step process that does not require particular conditions (i.e., low pH, controlled temperature, specific solvents, addition of other RONS scavengers) which are required, instead, in other tests.[72] When H_2O_2 is formed in excess, however, it may decompose the yellow copper(I) complex.[73] This limitation can be easily bypassed by properly diluting the sample before the analysis. Despite these advantages, the DMP assay has been rarely used to detect H_2O_2 in PTWS,[14,28] and its reliability and specificity still need to be fully validated.

The colorimetric detection of NO_2^- anions is less problematic. The reaction used almost exclusively in most aqueous media is the well-known Griess assay, in which NO_2^- anions react with sulphanilic acid to form a red–violet di-azo compound coupled with 1-naphthylamine.[74,75,84] The reaction has been successfully used to detect NO_2^- in PTWS of different compositions.[4,14,24,40,47] The accuracy of the method proved to be comparable with ion chromatography for NO_2^- in PTWS generated from double-distilled (dd) water.[24] However, a careful validation in PTWS generated from cell culture media is still lacking.

The colorimetric detection of NO_3^- in most media generally relies on their previous reduction to the more reactive NO_2^- ions; the Griess reaction is, thus, the most used assay also for nitrates in water media, including PTWS. A wide variety of reducing agents is used to achieve NO_3^--to-NO_2^- conversion even in the case of PTWS.[49] It must be stated, though, that this indirect

TABLE 1 List of the main colorimetric and fluorimetric assays used for H_2O_2, NO_2^- and NO_3^- in different liquids, with their limits

RONS	Liquid	Probe-method	Product	Reported assay limits	References
H_2O_2	Water, Phys, PBS	Titanyl sulphate-colorimetric	Yellow Peroxititanyl sulphate	Precipitation of Ti sulphate reagent in buffered solutions (>20 mM buffer); addition of sodium azide is required to avoid H_2O_2 decomposition by NO_2^- in acid condition	[27,48–56]
	Water, Phys, PBS, RL, DMEM, RPMI	Amplex red® and peroxidase-fluorimetric	Resorufin	Double step process; peroxidase is sensitive to light and can catalyse the oxidation of Amplex® Red also by peroxynitrite	[20,40,57–63]
	PBS, DMEM	Fe^{2+} xylenol-fluorimetric	Orange Fe^{3+} xylenol	Interferences from chemicals used in sample preparation (ascorbic acid, EDTA, heparin, DMSO, SDS, NP-40, Tris and ethanol); sensitivity to many other organic hydro-peroxides (–OOH) (possibly present in PTWS)	[64–66]
	Water, DMEM	Cu^{2+} and 2,9-dimethyl-1,10-phenanthroline (DMP)-colorimetric	Orange $Cu(DMP)_2^+$	excess of H_2O_2 may lead to destruction of the yellow copper(I) complex	[28,67–73]
NO_2^-	Water, Phys, PBS, RL, DMEM, RPMI	Griess reagents: sulphanilamide and napthyl-ethylene-diamine (NED) - colorimetric	Azo compound coupled with NED	Griess reagents compete for nitrite (minimised by adding the two components sequentially); possible interferences with NADPH (rarely present in PTWS)	[4,11,14,24,40,47,48,62,62,74–76]
NO_3^-	Water, Phys, PBS, RL, DMEM, RPMI	Nitrate Reductase or metallic Cd or V to reduce NO_3^- to NO_2^- and Griess reagents-colorimetric	Azo compound coupled with NED	Double-step process; nitrate reductase is unstable after reconstitution with buffer and is sensitive to cycles of freezing and thawing; Cd and V are toxic; possible interferences of other RONS with the reducing agent.	[11,49,75–77]
	Water, river water, sewage effluents	2.6-xylenol-colorimetric	4-nitro-2,6-xylenol	Require strong acidic conditions; possible interference of chlorides and glucose	[17,47,48,75,75,78–83]

Abbreviations: DMEM, Dulbecco's modified Eagle's medium; DMP, 2,9-dimethyl-1,10-phenanthroline; PB, phosphate-buffered solution; PBS, phosphate-buffered saline solution; Phys, physiologic solution; RL, Ringer's lactate solution; RONS, reactive oxygen and nitrogen species; RPMI, Roswell Park Memorial Institute medium.

approach is not very accurate in PTWS, since a systematic underestimation of the amount of nitrates can occur due to interferences in the reduction.[74,76,77]

An alternative method to directly detect NO_3^- in liquids is a colorimetric reaction based on the nitration of 2-6-xylenol to 4-nitro-2,6-xylenol, to be determined photometrically.[78,82] The method requires strong acid conditions (large excess of a sulphuric/phosphoric acid mixture) to promote the conversion of NO_3^- in nitronium ion NO_2^+, which is believed to be the main nitrating species.[79,82] The assay consists of a one-step process of 7–10 min per sample and has been successfully used for detecting nitrates in river water, estuary water and sewage.[83] In the case of PTWS, however, the method has been used rarely,[27,55] and the Griess assay after NO_3^- reduction to NO_2^- remains the most popular approach.

Following the considerations expressed above, it is our opinion that some of the presented colorimetric methods are of potential interest for detecting long-lived RONS, such as H_2O_2, NO_2^- and NO_3^- in PTWS generated from different liquids, including cell culture media. The research here presented, therefore, tests the reliability of such colorimetric assays in PTWS of complex composition, like those generated in cell culture media, where the detection of RONS is generally difficult due to the several organic/inorganic compounds present. Among all possible cell culture media, DMEM was chosen because it is one of the most used liquid to generate PTWS for biological applications and because its concentration of additives is one of the highest, compared to other cell culture media, representing one of the most tricky matrices for RONS detection.

In this research, we have used the DMP assay (scheme in Figure 1a) for the detection of H_2O_2, as an alternative to the widely diffused Amplex Red assay, whose limitations have been previously discussed. The efficacy of the Griess assay for NO_2^- detection (scheme in Figure 1b) was then validated in DMEM. Finally, the 2,6-xylenol nitration (scheme in Figure 1c) was exploited to detect NO_3^- ions as an alternative to the nitrate/nitrite Griess assay, reported to be quite inaccurate in nitrate detection, as previously discussed.

All the assays investigated were chosen because they consist of one simple and fast step, reactions (less than 10 min) that can be set with ready-to-use commercially

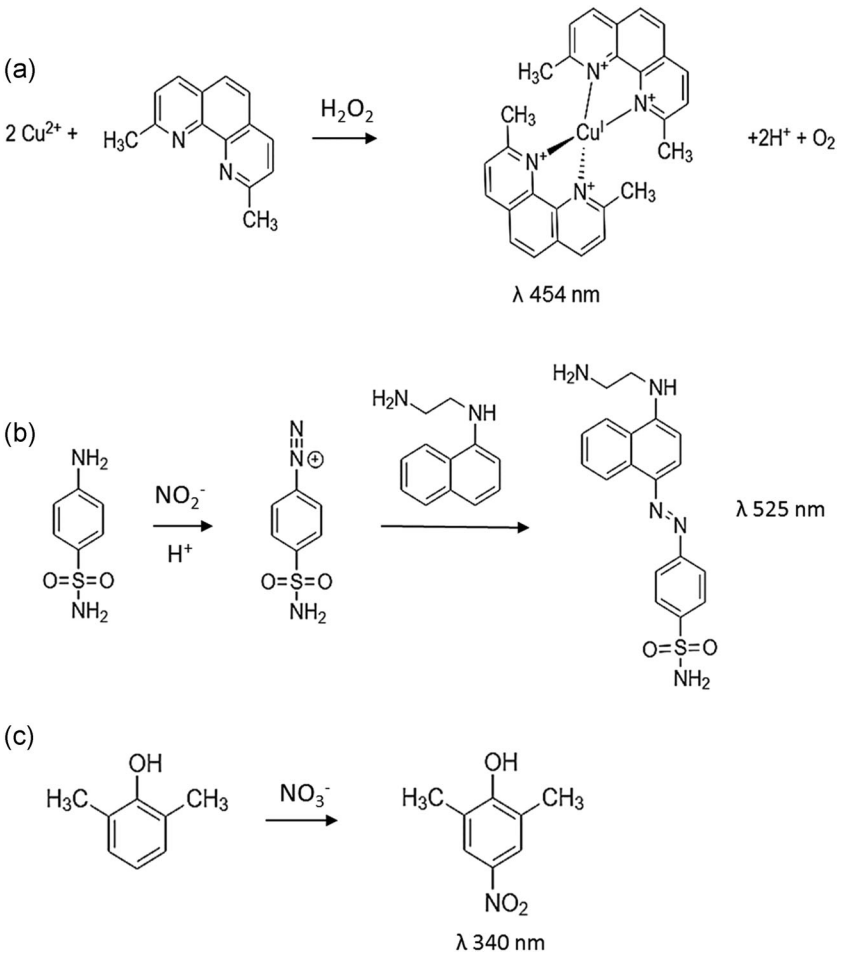

FIGURE 1 Chemical reactions at the base of colorimetric assays used for the detection of H_2O_2, NO_2^- and NO_3^- in water and in DMEM. (a) DMP (2,9-dimethyl-1,10-phenanthroline) assay to detect H_2O_2, (b) Griess assay to detect NO_2^- and (c) 2,6-xylenol assay to detect NO_3^-

available assay kits operating at room temperature, in a wide pH range. Each reaction, moreover, can be easily started directly in cuvettes, with a conventional spectrophotometer, and there is no need for sophisticated equipment. Robustness, linearity, accuracy and specificity of each reaction have been analysed in water and in DMEM with standard solutions of each RONS, whereas the effective possibility to use proposed reactions even in PTWS has been demonstrated for RONS plasma-generated in DMEM. The results reported here highlight the importance to validate the assays in each liquid tested. Moreover it is also important to check the whole visible spectrum (400–800 nm range) while using ready-to-use colorimetric assays. Manufacturers propose to acquire single absorbance reads at the suggested wavelength. In this way, it is possible to search for potential anomalies in the spectrum due to additional by-products formed by the reaction of reagent kits with other components in the media, and from changes in the shape/position of the analytical peak. The best way to operate would consist of testing the specificity of each method towards all possible RONS in PTWS, including transient ones. Nonetheless, owing to the nature of species like O_3, $ONOO^-$ and OH, this can be hard to perform. In addition, due to their short lifetime and to their great reactivity, the concentration of transient RONS in PTWS may be very low if compared to the concentration of stable RONS like H_2O_2, NO_2^- or NO_3^- (ranging from μM to mM). For these reasons, we focused our attention only on long-lived species (i.e., chlorides), which can be copresent with analysed RONS and interfere with their detection.

2 | EXPERIMENTAL SECTION

2.1 | Colorimetric assays for the detection of H_2O_2, NO_2^- and NO_3^-

The detection of H_2O_2, NO_2^- and NO_3^- RONS was carried out by using the commercial reagents listed in Table 2. Spectroquant® test kits (Merck) for spectrophotometric analysis are ready-to-use kits optimised for easy handling in routine and special analyses in water, food and environmental analytics.

The reliability of each colorimetric reaction was assessed in RONS standard solutions prepared in dd water or in DMEM (cat. N. D1145; Sigma-Aldrich) without phenol red, supplemented with 10% v/v fetal bovine serum (cat. N. F7524; Sigma-Aldrich), 2 mM L-glutamine (cat. N. G7513; Sigma-Aldrich), penicillin/streptomycin solution (20 units ml^{-1}/20 mg ml^{-1}, cat. N. T4049; Sigma-Aldrich). UV-Vis absorbance measurements were performed with a Cary 60 UV-Vis (Agilent) spectrophotometer in the 200–800 nm range, with a scan resolution of 1 nm. Disposable plastic cuvettes (cat. N. 223-9955; Bio-Rad) with a semimicro volume of 1 ml and 10 mm optical length were used for the spectrophotometric readings. The manufacturers recommend filtering turbid samples before the tests for H_2O_2 and NO_2^-, since these kits are thought to be used for wastewater analysis. No turbid samples, though, were formed in our research. In all experiments, the samples were analysed immediately at the end of the reaction time. For all measurements, the blank was prepared using dd water instead of the sample, according to the manufacturer's protocols. Samples with analyte concentrations exceeding the detection range were diluted with dd water before the measurements. In the same way, the sample was properly diluted so as to confine the absorbance intensity within 1 and grant the validity of Lambert–Beer law.

2.1.1 | Detection of H_2O_2

Hydrogen peroxide was detected by using the copper-phenanthroline assay (see Table 2). The commercial test kit consists of two numbered reagent bottles, whose composition is not exactly defined by the manufacturers, stored at +15/+25°C. Reagents are to be added to the sample starting from bottle 1. The manufacturer recommends adjusting the pH of the samples in the 4–10 range. Sixtyfive microliters each of reagents 1 and 2 were added to 1 ml of the sample directly in a 1 ml cuvette and left for 10 min (reaction time). Afterwards, the colour of the resulting solution to be analysed remained stable for 20 min. Standard solutions of H_2O_2 in the range 0–300 μM were prepared in dd water and in DMEM from a 30% w/w standard H_2O_2 water solution (cat. N. 95321; Sigma-Aldrich).

TABLE 2 Commercial reagent test kits used for colorimetric detection of H_2O_2, NO_2^- and NO_3^-

RONS	Commercial test kit	Principle	λ_{max} (nm)	Range	Indication
H_2O_2	Spectroquant® 1.18789.001, Merck	Copper-DMP assay	454	8–175 μM	Water
NO_2^-	Spectroquant® 1.14776.001, Merck	Griess assay	525	1.5–70 μM	Water
NO_3^-	Spectroquant® 1.09713.002, Merck	2,6-xylenol assay	340	0.1–1.8 mM	Water

Abbreviations: DMP, 2,9-dimethyl-1,10-phenanthroline; RONS, reactive oxygen and nitrogen species.

2.1.2 | Detection of NO_2^-

Nitrite ions were detected with the Griess assay (see Table 2). The commercial test kit consists of one reagent vial stored at +15/+25°C containing the undefined mixture reagents in powder. The manufacturers recommend to adjust the pH of the sample within the range of 2–10. The assay was performed as follows: 13 mg of the reagent mixture were added to 1 ml of the sample directly in a 1 ml volume cuvette; the mixture was then vigorously pipetted till the complete dissolution of the reagent powder and left to react for 10 min (reaction time). The colour of the measurement solution remained stable for 60 min. Standard solutions of nitrites were prepared in dd water and in DMEM from $NaNO_2$ (cat. N. S2252, purity ≥99.0%; Sigma-Aldrich). Nearly 0.050 g of $NaNO_2$ were dissolved in 500 ml of dd water to prepare a 2 mM mother solution, to be diluted in water or in DMEM for preparing solutions in the 0–220 μM range.

2.1.3 | Detection of NO_3^-

Nitrate ions were detected by using the 2,6-xylenol assay (see Table 2). The commercial test kit consists of two reagent bottles stored at 15–25°C, the first containing a solution of sulphuric and phosphoric acid, the second with the nitrate-sensitive probe. The assay was performed as follows: 2 ml of the sulphuric/phosphoric solution were transferred in a test tube; 250 μl of the sample were added without mixing, then 250 μl of reagent from bottle 2 were added to the mixture. The solution was vigorously shaken, then it became heated for the reaction. The system was then left reacting for 10 min (reaction time) without any cooling and analysed soon after. The colour of the measurement solutions remained stable for 30 min after the reaction. Standard nitrates solutions in the 0 to 1.6mM range were prepared in dd water and in DMEM by proper dilutions of a 16 mM standard nitrate solution for ion chromatography (cat. N. 74246; Honeywell Fluka).

2.2 | PTWS generation

PTWS were generated with a Dielectric Barrier Discharge (DBD) PetriPlas$^+$ plasma source, built by the Leibniz Institute for Plasma Science and Technologies (INP, Greifswald) and properly modified by coauthors of this paper. A scheme of the experimental apparatus is reported in Figure 2. The source is made of a Plexiglas flow unit set with gas connections and of a discharge unit. This latter consists of a stainless steel grounded mesh 4 mm far from a disc-shaped high-voltage copper electrode (3 cm diameter) covered with a dielectric glass disc (1 mm thick). A detailed description of the apparatus was published in our previous papers.[14,30] An electric field at 6 kHz frequency and 13.5 kV peak-to-peak voltage was applied to ignite the discharges, modulated in all experiments at a 25% duty cycle, 25 ms plasma on (t_{on}) over a period ($t = t_{on} + t_{off}$) of 100 ms.

Liquids were plasma-treated in 2 ml aliquots contained in a commercial TPP® Petri dish (57 mm diameter; Sigma-Aldrich) located below the discharge unit, 3 mm far from the discharge. During the treatments the Petri dish is sealed to the discharge unit, so the gap between the liquid and the discharge is not exposed to the atmosphere. Purging the gap with the gas feed before igniting the plasma allows to carefully control the chemical composition of the discharge. Pure O_2 or synthetic air,

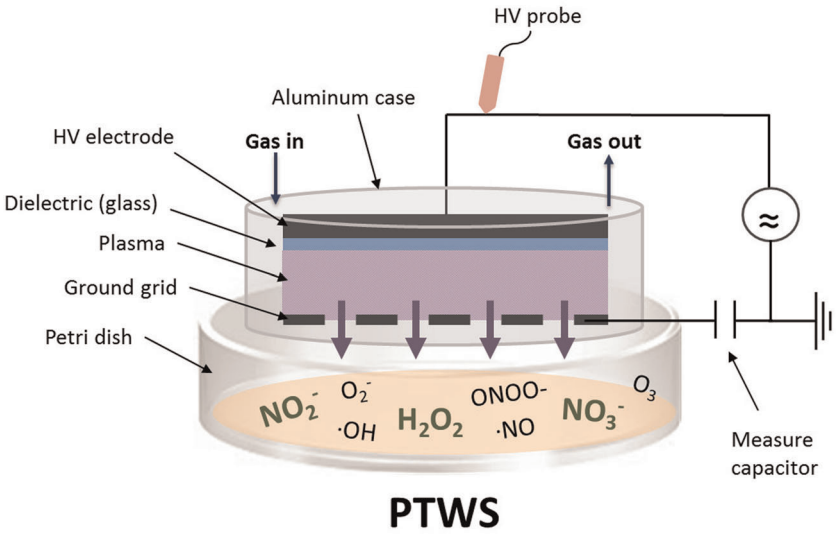

FIGURE 2 Schematic representation of DBD plasma source used to generate PTWS. Abbreviations: DBD, dielectric barrier discharge; HV, high-voltage; PTWS, plasma-treated water solution

both at 0.5 slm flow rate, were used to purge the chamber and feed the plasma during the treatments. In this way, the formation of nitrites could be promoted (in air-DBD), or excluded (in O_2-DBD) in PTWS. In each feed, the DBDs were ignited at different treatment times, from 60 to 300 s, for dosing the amount of RONS in the PTWS. The concentrations of NO_2^-, NO_3^- and H_2O_2 in the liquid were then evaluated by means of the colorimetric reactions investigated. None of the reagents of the colorimetric assays was added before treating liquids, to avoid potential modifications of the sensitive probes due to the plasma. If needed, PTWS were diluted with dd water before adding the reagents, to confine RONS concentration within the detection limits of each assay. Dilution was performed with dd water instead of untreated medium to avoid potential scavenging of the plasma-produced RONS. During the experiments, the pH of PTWS was measured after plasma treatment and before carrying on the colorimetric analyses.

2.3 | Data processing and statistical analysis

Baseline correction from acquired spectra was performed, when needed, with the Origin statistical software version Pro8. In the case of H_2O_2 detection in DMEM, as the analytical peak was generated also in H_2O_2-free DMEM, the signal of untreated DMEM was subtracted, after baseline correction, as it will be discussed. Accuracy, precision, limit of detection (LOD), linearity and specificity of each assay have been evaluated. Concentration/response relationships were evaluated by analysing a minimum of eight concentrations per assay. In the case of a linear relationship, a regression line was calculated with the least squares method to determine correlation coefficient (R^2), y-intercept and slope of regression (S). The calculated R^2 from the regression analysis was used as a mathematical estimator of linearity. LODs have been calculated from calibration curves, according to Equation (1), where SD_y is the y-intercept standard deviation and S is the slope of the regression line.

$$\mathrm{LOD} = 3.3 \times \frac{SD_y}{S}. \quad (1)$$

Control samples with a known concentration of each RONS in dd water and in DMEM were used to evaluate the precision and accuracy of the methods with at least five replicates. Precision, which is a degree of scatter between a series of measurements, was calculated as the percent relative standard deviation of each data set; accuracy, which expresses the closeness of agreement of measured values with the true values, was calculated as percent recovery of experimental concentration back-calculated from each calibration curve with respect to the known concentration. A qualitative evaluation of the specificity of each method was ultimately performed by analysing the response obtained in water and in DMEM solutions simultaneously containing the ROS or RNS of interest in presence of other RONS. Statistical significant differences between concentrations among samples were computed using the statistical software GraphPad Prism version 6.1. A one-way analysis of variance was performed with a subsequent Turkey's multiple comparisons test by assuming the normal distribution of the data. Statistic results of specificity tests were shown as histograms of the mean $\pm$ SD. All $p < .01$ were considered statistically significant.

3 | RESULTS AND DISCUSSION

Table 3 summarises the results obtained for the validation of the assays in dd water and in DMEM solutions of each RONS. Each case is discussed in the next paragraphs. The wavelength of absorption maxima (λ_{max}) registered in both liquids after each reaction in presence of the RONS of interest is reported to highlight the changes of λ_{max} in DMEM with respect to water. Slope, intercept, R^2 and LOD calculated from calibration curves for each RONS are shown, as well as accuracy and precision evaluated for the detection of each RONS in control solutions of known concentration.

The detection of each RONS in water and/or DMEM after plasma exposure will be shown in the following paragraphs. During the experiments, the pH of the liquids was measured after plasma treatment, before performing the colorimetric analyses. In the case of DMEM, due to the presence of a sodium bicarbonate buffer system (3.4 g/L), the pH of the medium is not altered after exposure to plasma and remains constant at 7.4. Concerning water, acidification of the liquid was found immediately after the end of the plasma treatment (pH 3.5). This acidification, however, should not interfere with the conditions to perform the colorimetric assays under an investigation. In fact, the 2,6-xylenol assay and Griess assay for the detection of NO_3^- and NO_2^- operate in acid condition once reagent mixtures are added to the samples (pH range within 2.0–2.5 for Griess assay and within 1.0–3.0 for 2,6-xylenol assay). In the case of H_2O_2 detection, then, the DMP assay is quite robust towards wide changes in the pH. Even if manufacturers indicate that the pH of the samples must be within 4–10 interval, from previous experiments, we confirmed that the DMP assay tolerates pH lower than 4. We treated water solutions of

TABLE 3 Results of statistical calculations after calibration of NO_2^-, NO_3- and H_2O_2 solutions in double-distilled (dd) water and Dulbecco's modifies Eagle's medium (DMEM)

	dd Water			DMEM		
	NO_2^-	NO_3^-	H_2O_2	NO_2^-	NO_3^-	H_2O_2
λ_{max} (nm)	525	340	455	525	505	455
Slope ± *SD*	0.0293 ± 0.0005	0.75 ± 0.03	0.0188 ± 0.0007	0.0287 ± 0.0005	0.71 ± 0.05	0.0085 ± 0.0002
Intercept ± *SD*	−0.07 ± 0.05	0.04 ± 0.02	−0.24 ± 0.12	−0.09 ± 0.05	0.08 ± 0.04	−0.01 ± 0.04
R^2	0.9973	0.9910	0.9888	0.9967	0.9652	0.9932
Limit of detection	6 μM	0.1 mM	22 μM	6 μM	0.2 mM	14 μM
Accuracy (%)	95	99	97	95	–	97
Precision (%)	4	4	4	6	–	14

organic molecules that required acid conditions to dissolve in water and we successfully used the DMP assay to detect H_2O_2 in these water solutions.

3.1 | H_2O_2 detection

In the presence of H_2O_2, the DMP assay leads to the formation of a red–orange complex $Cu(DMP)_2^+$ with a characteristic absorption peak at 455 nm. The peak is similar in shape and position for dd water (Figure 3a) and DMEM (Figure 3b), with absorption intensities proportional to the concentration of H_2O_2 in both liquids. In the case of DMEM, differently from dd water, the characteristic absorption peak is revealed even with no H_2O_2 added (black track in Figure 3b), probably generated by weak interferences of medium components with the reagents of the kit. To avoid that this initial contribution leads to an overestimation of H_2O_2 that would affect the accuracy of the test, the spectral contribution of DMEM (with the kit reagents added) was subtracted from the spectra of the H_2O_2-containing samples. After this subtraction, indeed, a linear trend of the signal at 455 nm is obtained as a function of the H_2O_2 concentration in DMEM (Figure 3d, red line) as well as in dd water (Figure 3d, black line). Correlation coefficients, slope and intercept of the regression curves for both liquids are shown in Table 3. An LOD of 22 μM in dd water and of 15 μM in DMEM was calculated. The greater sensitivity of the test in DMEM rather than in water is generated as a consequence of the higher standard deviation calculated for the intercept of the calibration curve in water ($SD = 0.12$, Table 3) rather than in DMEM ($SD = 0.04$, Table 3), in spite of an opposite trend in case of the slopes of the curves, found higher in water than in DMEM (see Table 3). A part from calculations, however, we do not believe that DMEM may possess some chemical characteristic that could increase the sensitivity of the method.

H_2O_2 solutions with a known concentration (100 μM) in dd water and in DMEM were used as quality controls, for the calculation of accuracy and precision (Table 3). In both liquids a percent accuracy higher than 95% was calculated; in DMEM the test proved to be less precise with higher error bars than the ones found in the water series.

The specificity of the test for H_2O_2 was evaluated by comparing the spectroscopic signals generated in solutions of H_2O_2 (300 μM), NO_2^- (200 μM) and NO_3^- (0.8 mM), alone and mixed among each other, to simulate PTWS of different compositions. The results of the specificity test, presented in Figure 3e, show that the spectroscopic signal of H_2O_2 at the calculated concentration appears only when H_2O_2 is actually present in the liquids. Solutions of NO_2^- or NO_3^- alone do not produce any signal after the addition of the reagents kit, confirming that the DMP assay is selective for H_2O_2 in dd water (Figure 3e, grey bars) as well as in DMEM (Figure 3e, red bars). In addition, NO_2^- and NO_3^- (alone or in a mixture) do not seem to interfere with the detection of H_2O_2 present in the solution at the same time, as the signal appears neither amplified nor depressed and the calculated concentrations of H_2O_2 alone or in presence of the other RONS are not statistically different.

No particular interfering species is mentioned in the literature for this assay. Manufacturers report, however, that many molecules could alter H_2O_2 detection, such as ascorbate, citrate, peracetic acid and chlorides (>0.1% w/w), among others. Of these interfering species, indeed, only chlorides are present in DMEM in high concentrations (6.4 g/L, about 0.7% w/w); the interference that could develop in presence of a high amount of chlorides is not described by the

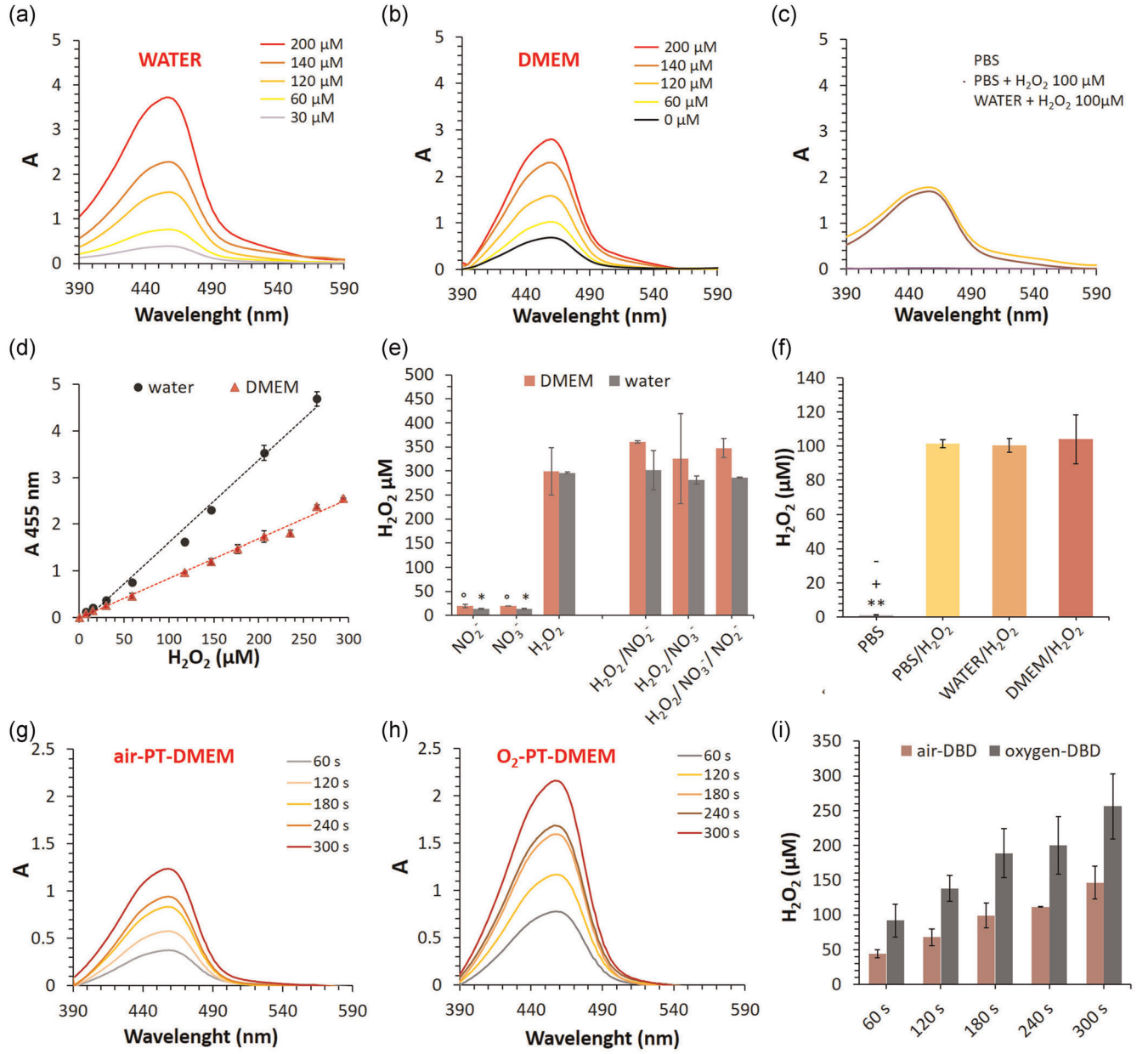

FIGURE 3 Spectroscopic signals after the copper-DMP assay in H_2O_2 solutions at different concentrations (a) in dd water and (b) in DMEM. (c) spectroscopic signals after the DMP assay in H_2O_2 (100 µM) solutions in dd water and in PBS; (d) scatter plot of the signal as a function of H_2O_2 concentration in water and in DMEM with calculated regression lines; (e) H_2O_2 concentration values elaborated from signals detected in solutions of different RONS in dd water and in DMEM; (f) H_2O_2 concentration values elaborated from signals detected in PBS as it and in H_2O_2 (100 µM) solutions in dd water, in PBS and in DMEM; signals detected after the DMP assay in PT-DMEM treated with (g) air- and (h) O_2-fed DBD as a function of the treatment time (60-300 s); (i) calculated H_2O_2 concentrations in PT-DMEM after O_2- and air-fed DBD as a function of treatment time. One-way ANOVA + Tukey's post test: $^{\circ}p < .01$ versus 'H_2O_2' in DMEM series (red bars) and $^{*}p < .01$ versus 'H_2O_2' in water series (grey bars) in the graph (e); $^{-}p < .01$ versus 'PBS/H_2O_2,' $^{+}p < .01$ versus 'WATER/H_2O_2' and $^{**}p < .01$ versus 'DMEM/H_2O_2' in the graph (f). Abbreviations: ANOVA, analysis of variance; DBD, dielectric barrier discharge; DMEM, Dulbecco's modified Eagle's medium; DMP, 2,9-dimethyl-1,10-phenanthroline; dd, double-distilled; PBS, phosphate-buffered saline solution; PT, plasma-treated; RONS, reactive oxygen and nitrogen species

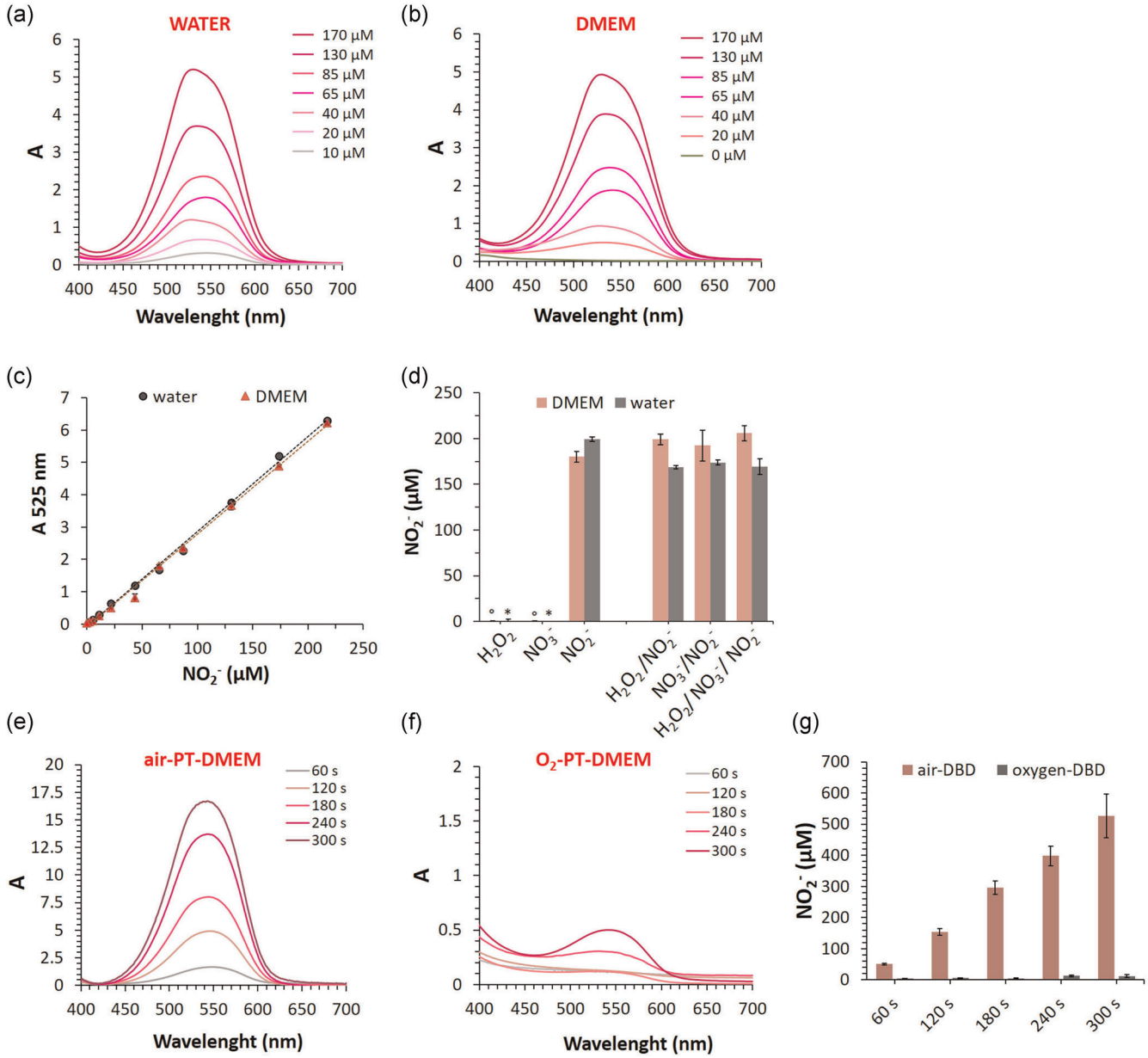

FIGURE 4 Spectroscopic signals after the Griess assay in NO_2^- solutions (a) in dd water and (b) in DMEM. (c) Scatter plot of the signal as a function of NO_2^- concentration in dd water and in DMEM with calculated regression lines; (d) NO_2^- concentration values elaborated from signals detected in RONS solutions in dd water and in DMEM; signals detected after the Griess assay in PT-DMEM with (e) air- and with (f) O_2-fed DBD as a function of the treatment time (60–300 s); (g) NO_2^- concentrations calculated in PTWS generated in DMEM after O_2- and air-fed DBDs as a function of treatment time. One-way analysis of variance + Tukey's post test: °$p < .01$ versus 'NO_2^-' in DMEM series (red bars) and *$p < .01$ versus 'NO_2^-' in water series (grey bars) in the graph (d). Abbreviations: DBD, Dielectric Barrier Discharge; DMEM, Dulbecco's modified Eagle's medium; dd, double-distilled; PT, plasma-treated; RONS, reactive oxygen and nitrogen species

manufacturers. For these reasons, we have investigated the detection of H_2O_2 with DMP also in PBS, a buffered solution containing 8.20 g/L (about 0.82% w/w) of chlorides. As reported in Figure 3c, the spectroscopic signals acquired in dd water (red spectra) and in PBS (grey spectra) containing the same amount of H_2O_2 (100 µM) overlap perfectly. No interactions of DMP reagents with chlorides were detected even in absence of H_2O_2, as the addition of DMP reagent in PBS alone did not result in any peak (Figure 3c, PBS, violet track). The concentrations for H_2O_2 in PBS (yellow bar, Figure 3f), in dd water (orange bar, Figure 3f) and in DMEM (orange bar, Figure 3f), resulted not significantly different. Under these conditions, thus, it is possible to conclude that no interference due to chlorides should result in H_2O_2

detection for media with chlorides up to 0.8% w/w, as DMEM.

With the precautions reported above, the DMP assay can be successfully adapted to the detection of H_2O_2 in a liquid with a complex composition, such as DMEM, where the test maintains its linearity, accuracy and selectivity and confirms to be a simple, fast and robust method. The DMP assay was also tested in PT-DMEM, where the presence of stable and transient RONS continuously produced in the medium and of plasma-modified organic components, is an additional degree of complexity.

PTWS have been generated in 2 ml of DMEM with air- and O_2-fed DBD at increasing treatment times, from 60 to 300 s. Due to the presence of a buffering system in DMEM, the pH of the medium was not altered after plasma exposure. The spectroscopic signals revealed by the DMP assay after each treatment (within 10 min after the treatment) are shown in Figure 3g for PT-DMEM treated in air-fed DBDs and in Figure 3h for PT-DMEM treated in O_2-fed DBDs. No difference in terms of peak shape and position was found in comparison with the signals generated in untreated solutions of H_2O_2 in DMEM (Figure 3b). H_2O_2 concentration was thus back-calculated through regression lines obtained by H_2O_2 calibration in DMEM (Figure 3d, red line). The calculated concentrations of H_2O_2 in PT-DMEM are reported in Figure 3i. As expected, the H_2O_2 concentration was found higher in O_2-treated with respect to air-treated PTWS, where oxygenated species in the plasma phase are reasonably also involved in the oxidation of nitrogen species to produce transient and stable RNS, as it will be discussed in Section 3.2. Moreover, the calculated concentration of H_2O_2 in PTWS was found increasing, as a function of treatment time, in both O_2- and air-treated DMEM, as expected. The concentrations of H_2O_2 in PT-DMEM measured with the DMP assay are, therefore, quite in accordance with those expected according to plasma conditions used to generate the tested PTWS.

3.2 | NO_2^- detection

The spectra acquired in NO_2^- standard solutions in dd water and in DMEM after the Griess assay are reported in Figure 4a,b. The reaction in the presence of NO_2^- forms a red-violet azo dye with a characteristic absorption peak at 525 nm, similar in shape and position in dd water (Figure 4a) and in DMEM (Figure 4b). In both cases, the intensity of the peak increases with the concentration of NO_2^-. In the case of nitrite-free DMEM (grey line in Figure 4b) no absorption peak is revealed, attesting the lack of potential interferences by medium components. It is, therefore, possible to observe a linear trend of the signal at 525 nm with the concentration of NO_2^- in DMEM (Figure 4c, red data points) as well as in water (Figure 4c, black data points). The regression analysis confirms the linearity of the trends in DMEM (Figure 4c, red line) and in water (Figure 4c, black line). Correlation coefficients, slope and intercept of the regression lines calculated for both liquids are shown in Table 3. The experimental LOD calculated in water and in DMEM in our experimental conditions is about 6 μM.

Nitrite solutions with a known concentration (100 μM) in water and DMEM were used as control samples to calculate the accuracy and precision of the test (Table 2). In both liquids, the test showed similar percent accuracy, higher than 95% and similar precision, 4% and 6% in water and in DMEM, respectively. As for the case of H_2O_2 presented previously, also the specificity of the Griess assay for nitrite ions was evaluated by comparing the spectroscopic signals generated in solutions of H_2O_2 (300 μM), NO_2^- (200 μM) and NO_3^- (0.8 mM), alone or in the mixture. The results of the specificity test are shown in Figure 4d. No NO_2^- signal could be revealed in solutions of H_2O_2 or NO_3^- alone, confirming the selectivity of the Griess assay for NO_2^- in water (Figure 4d, grey bars) as well as in DMEM (Figure 4d, red bars). In addition, the detection of NO_2^- resulted not influenced by the simultaneous presence of H_2O_2 and/or NO_3^- (alone or in mixture) in solution, since the NO_2^- signal was neither amplified nor depressed in water and in DMEM in presence of the other RONS. Likely this occurs because, at such low concentrations, the reaction of NO_2^- with H_2O_2 is much slower compared to the one obtained with the colorimetric reagents, which are added in large excess.[52]

Following these considerations, we can state that also the Griess assay successfully adapts to the detection of NO_2^- in a liquid with a complex composition, such as DMEM, since the test maintains its linearity, accuracy and selectivity in the medium. The assay was thus tested in PTWS DBD-generated in DMEM, to assess whether the presence of transient RONS in the medium and/or of plasma-modified organic compounds may challenge the reliability of the detection.

PTWS were generated in 2-ml samples of DMEM with air- and O_2-fed DBDs at increasing treatment times, from 60 to 300 s. Due to the presence of a buffering system in DMEM, the pH of the medium was not altered after plasma exposure. The spectroscopic signals generated after the Griess assay in PT-DMEM are shown in Figure 4e,f. As for the previous case of H_2O_2, no difference in terms of peak shape and position was found in comparison with the signals generated in untreated solutions of NO_2^- in DMEM (Figure 4b). The

NO_2^- concentration was thus back-calculated by using the regression lines obtained in DMEM (Figure 4c, red line). As expected, the NO_2^- concentration was found very high (up to 500 μM) in air-treated DMEM, where both oxygen and nitrogen precursors, required for the formation of NO_2^- ions, are present in the plasma, whereas nitrites were almost zero in O_2-treated PTWS because of the lack of nitrogen precursors in the plasma when only O_2 is fed. The calculated concentrations of NO_2^- increase as a function of treatment time in air-treated DMEM, as expected. The concentrations of NO_2^- in PT-DMEM measured with the Griess assay were, therefore, found quite in accordance with those expected.

3.3 | NO_3^- detection

The UV-VIS spectra acquired in NO_3^- standard solutions in dd water and in DMEM after the 2,6-xylenol assay are reported in Figures 5a and 5b, respectively. The formation of 4-nitro-2,6-xylenol due to NO_3^- reacting with 2,6-xylenol in dd water was confirmed by the characteristic absorption track, with a primary peak at 340 nm and a weak secondary peak at about 500 nm (Figure 5a). The absorption intensity of the 340 nm peak was found to increase with the concentration of NO_3^- in water; a linear intensity trend of the signal was observed in water (Figure 5d, black data point) as a function of the NO_3^- concentration, confirmed by regression analysis (Figure 5d, black line), whose correlation coefficient, slope and intercept are listed in Table 3.

The LOD calculated (0.1 mM) was found in agreement with the one indicated by the manufacturers, 0.1 mM and the analysis of control samples (0.8 mM NO_3^- in water) has demonstrated high accuracy (99%) and precision (4%) for the test in water. The specificity of the test for nitrates in water was evaluated by comparing the spectroscopic signal at 340 nm generated in solutions of H_2O_2 (300 μM), NO_2^- (200 μM) and NO_3^- (0.8 mM), alone and mixed, to simulate PTWS of different compositions. The results of the specificity test (Figure 5e) show that the spectroscopic signal was found absent after the colorimetric assay in nitrate-free H_2O_2 and NO_2^- water solutions, whereas it was strong in solutions where the NO_3^- ions were present. Moreover, the detection of NO_3^- resulted not influenced by the simultaneous presence of H_2O_2 and/or NO_2^- in the solution, thus attesting the absence of cross interferences of the other RONS in NO_3^- detection by 2,6-xylenol assay.

Data obtained in DMEM analyses were quite different from the ones obtained in water. An absorption peak was generated also in DMEM after the assay in NO_3^- solutions, whose intensity increased with the concentration of NO_3^- (Figure 5b). A linear trend was registered between absorption intensities and nitrate concentration (Figure 5d, red data point), confirmed also by regression analysis performed on calibration data (Figure 5d, red line). The correlation coefficient, slope and intercept of the calibration curve calculated for the test in DMEM are listed in Table 3. In addition to these finding, however, the position of the absorption peak was found different from the one found in water experiments because it was found shifted from 340 to 500 nm (Figure 5b). The shift in the absorption peak is also confirmed by visual inspection of the samples (Figure 5f,g): the DMP reaction performed in water leads to a colourless solution, whereas in DMEM, a red-purple colour is observed, with intensity depending on the concentration of nitrates.

Concerning potential interfering compounds, manufacturers report that several metal ions, chlorides (>0.1% w/w) and organic compounds like D-glucose (>0.5 g/L) could alter the detection. Among the compounds listed, high concentrations of chlorides (6.4 g/L, about 0.7% w/w) and of D-glucose (4.5 g/L) in DMEM could be responsible for the observed red shift in the track. To test this hypothesis, nitrates were analysed with the 2,6-xylenol assay also in PBS, where the amount of chlorides is 0.82% w/w and in a water solution of D-glucose with the same concentration reported in DMEM (4.5 g/L), with and without the addition of NO_3^- to a final concentration of 0.8 mM. Indeed, the shift of the absorption peak from 340 nm (NO_3^- in water, Figure 5c, black track) to 500 nm was observed also in PBS (Figure 5c, NO_3^- in PBS red track). By comparing this spectrum with that recorded in PBS alone (Figure 5c, blue track), it is clear that the red shift is observed only when also NO_3^- is present in PBS, whereas no peak is detected in PBS alone. It is, therefore, reasonable to assume that chlorides may interfere in reactions with the nitrate ions or with the 4-nitro-xylenol product.

It is reported that, under the acid conditions of the assay, chlorides could reduce NO_3^- ions to nitrosyl chloride, which, in turn, would react with 2,6-xylenol to form 4-nitroso-2,6-xylenol. This reaction may lead, indeed, to the loss of the peak observed at 340 nm.[78,79,81] In the case of the formation of 4-nitroso-2,6-xylenol, however, a shift in peak position towards shorter wavelengths is reported,[78,79,81] in contrast with the bathochromic shift of the peak registered, instead, in our experiments.

In alkaline conditions, the observed red shift could be ascribed to the formation of phenolate anions,[85] but this is quite unlikely since the 2,6-xylenol assay is performed in very strong acid conditions. In fact, although PBS and DMEM are solutions buffered at slightly basic pH, the sulphuric/phosphoric acid solution included in the

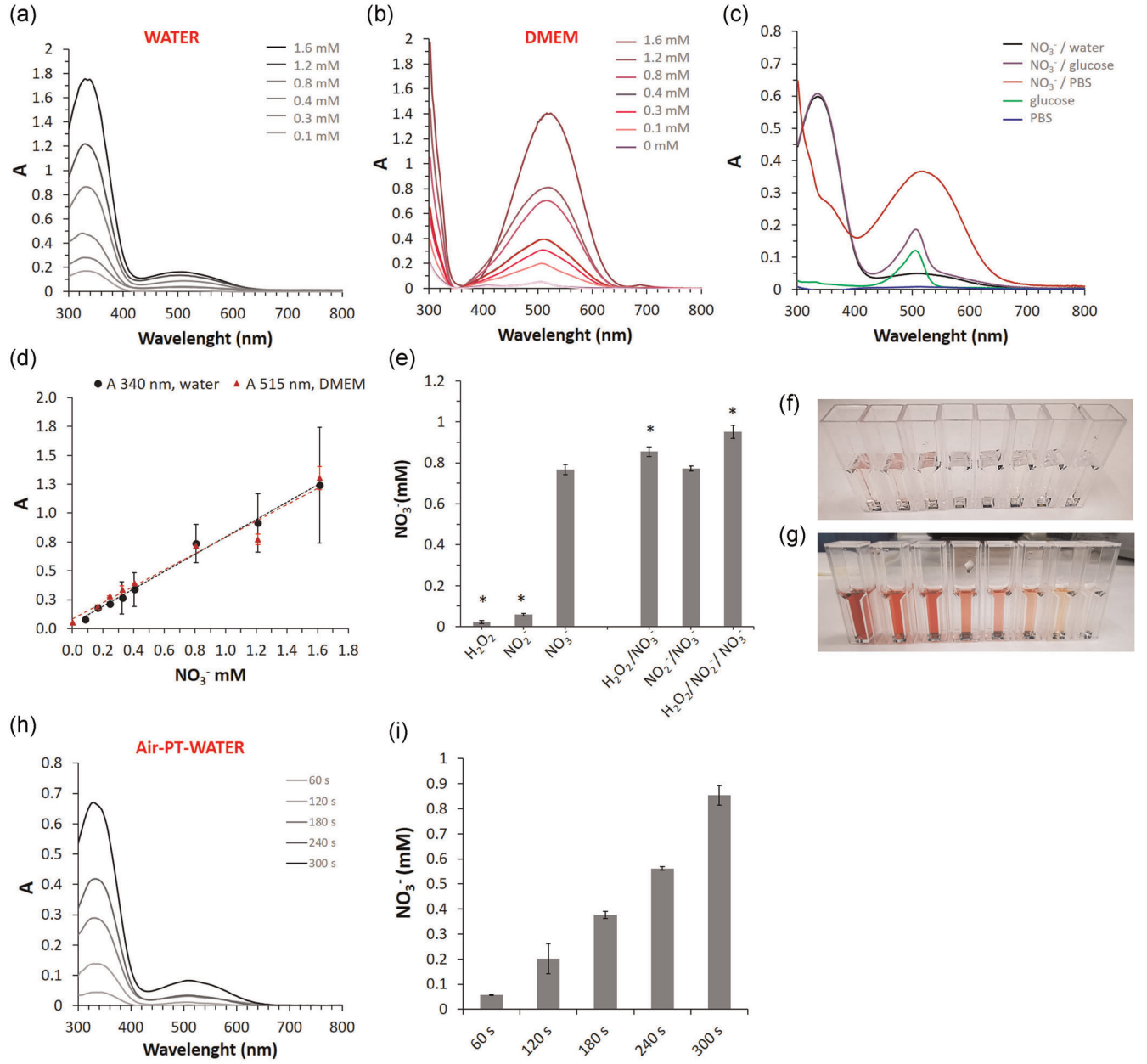

FIGURE 5 Spectroscopic signals after the 2,6-xylenol assay in NO_3^- in solutions (a) in water, (b) in DMEM. (c) signals after 2,6-xylenol assay in NO_3^- solutions prepared in dd water, in a water solution of D-glucose (4.5 g/L) and in PBS; (d) Scatter plot of the signal as a function of NO_3^- concentration in water and in DMEM with calculated regression lines; (e) NO_3^- concentration values elaborated from signals detected in RONS solutions in water; (f) photo of standard solutions of NO_3^- in water after performing the 2,6-xylenol assay (almost colourless); (g) photo of standard solutions of NO_3^- in DMEM after performing the 2,6-xylenol assay (red-purple colour with intensity depending on the NO_3^- concentration); (h) spectroscopic signals after the 2,6-xylenol assay in PT-dd water after air-DBD ignited for different treatment times (60–300 s); (i) NO_3^- concentration values calculated in PT-dd water as a function of treatment time in air-DBDs; One-way analysis of variance + Tukey's post test: *p <.001 versus 'NO_3^-' in (e). Abbreviations: DBD, dielectric barrier discharge; DMEM, Dulbecco's modified Eagle's medium; dd, double-distilled; PBS, phosphate-buffered saline solution; PT, plasma-treated; RONS, reactive oxygen and nitrogen species

2,6-xylenol assay is added in strong excess (2 ml) in comparison with the amount of DMEM or PBS sample (250 μl). It is therefore quite unlikely that buffer systems in PBS or DMEM can compensate the high excess of the acid mixture of the kit.

The presence of D-glucose in the assay formed a weak signal at 500 nm (Figure 5c, purple track), which remained even in absence of NO_3^- (Figure 5c, green-track), where no absorption at 340 nm was present. When NO_3^- ions were added, however, the signal at 340 nm remained still present with no shift, together with a weak signal at 500 nm, similar to the one detected in the nitrate-free glucose solution. Other than contributing to the absorption peak registered at 500 nm, the presence of D-glucose in the medium can be assumed not to be involved in the shift.

We could, thus, not identify the actual reason for the observed red shift of the 340 nm peak in DMEM; we believe, though, that it could be somehow related to the presence of chlorides. Although the linearity of the peak intensity with the concentration of nitrates was retained in spite of the shift of the peak to 500 nm, the stability of its colour was found lower than that of the peak at 340 nm. In the case of DMEM, an increase in the colour intensity after 2,6-xylenol assay was observed beyond the reaction time, whereas, in the case of water, the colour of the solutions remained stable up to 60 min, according to the indication of the manufacturers. As long as the samples are analysed immediately after the reaction time, in effect, the increase in signal intensity in the medium can be avoided, even if it must be representative of time-dependent reactions between assay products or reagents and components of DMEM that could also interfere in the NO_3^- detection.

Following these considerations, we can state that the 2,6-xylenol assay can be successfully used for the detection of NO_3^- in dd water simultaneously containing other RONS, with high accuracy and specificity for nitrates. On the contrary, in the case of cell culture media like DMEM, the reliability of the test is uncertain since the reaction product of nitrates with 2,6-xylenol is affected by some components of the medium, such as chlorides and glucose. It is, therefore, our opinion that further studies should be run to better understand the nature and the stability of the assay products over time in the case of DMEM, to ultimately validate the 2,6-xylenol method for nitrates also in PT-DMEM, where the detection could be affected by artefacts more than in untreated medium.

For these reasons, the 2,6-xylenol assay was not tested to quantify NO_3^- ions in PT-DMEM, as it was shown in the case of H_2O_2 and NO_2^- analysis; whereas it was tested in PT-dd water, where transient RONS, different from NO_2^- or H_2O_2, could anyway interfere in the detection. For this purpose, 2 ml of dd water were treated with air- DBDs ignited for different times, from 60 to 300 s. The spectroscopic signals generated by the 2,6-xylenol assay in PT-dd water are shown in Figure 5h. No difference in terms of peak shape and position was found in comparison with the signals generated in the untreated water solutions of NO_3^- (Figure 5a). The concentration of NO_3^- in PT-dd water was, thus, back-calculated by using the calibration curves for nitrates elaborated for water (Figure 5d, black line). As expected, the NO_3^- concentration was found very high (in mM range) in air-treated dd water, as both oxygen and nitrogen precursors required for forming the NO_3^- ions are present in the plasma, as for nitrites. The calculated concentrations of NO_3^- (Figure 5i) increase as a function of treatment time in air-treated dd water as well, as expected. According to the evidence, we can confirm the validity of the 2,6-xylenol to quantify NO_3^- ions in PT-dd water.

4 | CONCLUSION

The detection of RONS in untreated and plasma-treated cell culture media is challenged by the presence at the same time of several different compounds, organic and inorganic; on the other side, however, a careful balance of their chemical properties is required to targeting biological effects for clinical applications. For current and future research in the biomedical fields, it is therefore fundamental to count on accurate and reliable RONS detection methods also for complex biological matrices. Colorimetric assays offer simple and ready-to-use methods but also need to be accurately validated for the specific case to avoid artefacts and inaccuracy.

Here, the reliability of simple and fast colorimetric assays for the most common RONS, H_2O_2, NO_2^- and NO_3^-, found in PTWS of typical composition was investigated. The validity of each method was assessed for the first time in a complex biological liquid such as DMEM, a cell culture medium frequently used in Plasma Medicine to generate PTWS for in vitro cell growth and other biological experiments. The analytical studies performed proved the robustness and the accuracy of the DMP and of the Griess colorimetric assays in the detection, respectively, of H_2O_2 and NO_2^- in water as well as in DMEM. Such reactions proved to be selective for each specific RONS in water and in DMEM and, therefore, of potential interest for PTWS.

Indeed, the DMP assay for H_2O_2 and the Griess assay for NO_2^- were confirmed valid without modifications

also in the case of PT-DMEM generated in DBDs fed with O_2 or air. The amounts of NO_2^- and H_2O_2 found in PT-DMEM were in accordance with the plasma conditions used. It is, therefore, our opinion that the DMP assay and the Griess assay should be, respectively, used in the detection of H_2O_2 and NO_2^- in PTWS generated in liquids like PT-DMEM, for their valuable tolerance to high concentrations of inorganic and organic compounds.

The 2,6-xylenol assay successfully adapted to the detection of NO_3^- in dd water even in presence of other potentially competing RONS with high accuracy and specificity. This assay was confirmed valid also in PT-dd water generated after treatment with air-DBDs. The test allowed the quantification of high amounts of nitrates, in the mM range, increasing in the liquid as the DBD treatment time. In the case of DMEM, however, the 2,6-xylenol assay was affected by interferences causing a red shift in the absorption peak, whose nature could not be fully explained. We, thus, suggest that the 2,6-xylenol assay should be avoided for the detection of NO_3^- ions in PT-DMEM, until further studies are performed to identify the nature of the interferences, probably due to high amounts of chlorides and glucose in the medium.

It is very important to develop accurate and reliable detection methods that match the need for rapid accurate results also in complex biological liquids, through which redox drugs and RONS could be administrated to living tissues. The results reported here highlight the importance to thoroughly check the reliability of RONS detection methods and, when possible, to improve them, for all liquid vectors of RONS of potential interest in the biomedical field, including plasma-treated media. By following the approach described in this paper, for example, we could measure precisely the concentration of H_2O_2 and NO_2^- species in PT-DMEM generated in different plasma conditions and highlight, consequently, that precise proportions in H_2O_2 and NO_2^- are involved in increasing the selectivity of anticancer effects of PT-DMEM; indeed, a synergistic effect of NO_2^- in selectively decreasing the cytotoxic threshold of H_2O_2 on osteosarcoma cancer cells was found, whereas the same concentration of RONS was ineffective on endothelial nonmalignant cells.[30]

ACKNOWLEDGEMENTS

We thank K-D Weltmann and M. Schmidt (Leibniz Institute for Plasma Science and Technology, INP, Greifswald, Germany) for the cooperation offered with the development of the Petriplus+ plasma source. S. Cosmai (CNR-NANOTEC) and D. Benedetti (University of Bari Aldo Moro) are gratefully acknowledged for their technical support. This study was funded by the financial support of Regione Puglia, under grants 'LIPP' (grant no. 51, within the Framework Programme Agreement APQ 'Ricerca Scientifica', II atto integrative—Reti di Laboratori Pubblici di Ricerca) and of intra-Institute project CNR-NANOTEC SEED.

CONFLICT OF INTERESTS

The authors have declared that there are no conflict of interests.

AUTHOR CONTRIBUTIONS

Valeria Veronico was involved in conceptualisation, investigation, writing the original draft and review editing. Francesco Fracassi, Pietro Favia and Eloisa Sardella were involved in fund acquisition, Eloisa Sardella was involved in conceptualization and data curing. Eloisa Sardella, Pietro Favia and Roberto Gristina were involved in review editing.

DATA AVAILABILITY STATEMENT

The data that support the findings of this study are available from the corresponding author upon reasonable request.

ORCID

Eloisa Sardella http://orcid.org/0000-0002-6776-8327

REFERENCES

[1] K. Weltmann, F. Kolb, M. Holub, D. Uhrlandt, M. Šimek, K. Ostrikov, S. Hamaguchi, U. Cvelbar, M. Černák, B. Locke, A. Fridman, P. Favia, K. Becker, *Plasma Processes Polym.* **2019**, *16*(*1*), 1800118.

[2] I. Trizio, M. Garzia Trulli, C. Lo Porto, D. Pignatelli, G. Camporeale, F. Palumbo, E. Sardella, R. Gristina, P. Favia, in *Reference Module in Chemistry, Molecular Sciences and Chemical Engineering*, Elsevier, Waltham, MA **2018**.

[3] E. Sardella, F. Palumbo, G. Camporeale, P. Favia, *Materials* **2016**, *9*, 515.

[4] E. Sardella, M. G. Mola, R. Gristina, M. Piccione, V. Veronico, M. De Bellis, A. Cibelli, M. Buttiglione, V. Armenise, P. Favia, G. P. Nicchia, *Int. J. Mol. Sci.* **2020**, *21*(*9*), 3343.

[5] M. Laroussi, *Plasma Processes Polym.* **2014**, *11*(*12*), 1138.

[6] P. Favia, E. Sardella, H. Tanaka, *Plasma Processes Polym.* **2020**, *17*(*10*), 2070028.

[7] P. Ranieri, N. Sponsel, J. Kizer, M. Rojas-Pierce, R. Hernàndez, L. Gatiboni, A. Grunden, K. Stapelmann, *Plasma Processes Polym.* **2021**, *18*(*1*), 2000162.

[8] D. B. Graves, *J. Phys. Appl. Phys* **2012**, *45*(*26*), 263001.

[9] K. Wende, T. von Woedtke, K.D. Weltmann, S. Bekeschus, *Biol. Chem.* **2018**, *400*(*1*), 19.

[10] Y. Gorbanev, D. O'Connell, V. Chechik, *Chem. Eur. J.* **2016**, *22*(*10*), 3496.

[11] H. Tanaka, K. Nakamura, M. Mizuno, K. Ishikawa, K. Takeda, H. Kajiyama, F. Utsumi, F. Kikkawa, M. Hori, *Sci. Rep.* **2016**, *6*(*1*), 36282.

[12] S. Ikawa, K. Kitano, S. Hamaguchi, *Plasma Processes Polym.* **2010**, *7*(*1*), 33.

[13] Z. Machala, B. Tarabová, D. Sersenová, M. Janda, K. Hensel, *J. Phys. Appl. Phys* **2019**, *52*(*3*), 034002.
[14] A. Azzariti, R. M. Iacobazzi, R. Di Fonte, L. Porcelli, R. Gristina, P. Favia, F. Fracassi, I. Trizio, N. Silvestris, G. Guida, S. Tommasi, E. Sardella, *Sci. Rep.* **2019**, *9*(*1*), 4099.
[15] G. Bauer, D. Sersenová, D. B. Graves, Z. Machala, *Sci. Rep.* **2019**, *9*(*1*), 14210.
[16] G. Bauer, *Plasma Med.* **2019**, *9*(*1*), 57.
[17] I. Trizio, V. Rizzi, R. Gristina, E. Sardella, P. Cosma, E. Francioso, T. von Woedtke, P. Favia, *Plasma Processes Polym.* **2017**, *14*(*11*), 1700014.
[18] E. Biscop, A. Lin, W. van Boxem, J. van Loenhout, J. de Backer, C. Deben, S. Dewilde, E. Smits, A. Bogaerts, *Cancers* **2019**, *11*(*9*), 1287.
[19] D. Yan, A. Talbot, N. Nourmohammadi, X. Cheng, J. Canady, J. Sherman, M. Keidar, *Sci. Rep.* **2015**, *5*(*1*), 18339.
[20] S. Mohades, N. Barekzi, H. Razavi, V. Maruthamuthu, M. Laroussi, *Plasma Processes Polym.* **2016**, *13*(*12*), 1206.
[21] D. Koensgen, I. Besic, D. Gümbel, A. Kaul, M. Weiss, K. Diesin, A. Kramer, S. Bekeschus, A. Mustea, M. B. Stope, *Anticancer Res.* **2017**, *37*(*12*), 6739.
[22] G. Bauer, *Redox Biol.* **2019**, *26*, 101301.
[23] G. Bauer, *Mech. Ageing Dev.* **2018**, *172*, 59.
[24] B. Tarabová, P. Lukeš, M. Janda, K. Hensel, L. Šikurová, Z. Machala, *Plasma Processes Polym.* **2018**, *15*(*6*), 1800030.
[25] E. Freund, K. R. Liedtke, R. Gebbe, A. K. Heidecke, L.I. Partecke, S. Bekeschus, *IEEE Trans. Radiat. Plasma Med. Sci.* **2019**, *3*(*5*), 588.
[26] H. Tanaka, S. Bekeschus, D. Yan, M. Hori, M. Keidar, M. Laroussi, *Cancers* **2021**, *13*(*7*), 1737.
[27] K. Oehmigen, M. Hähnel, R. Brandenburg, C. Wilke, K. D. Weltmann, T. Woedtke, *Plasma Processes Polym.* **2010**, *7*(*3–4*), 250.
[28] P. Ranieri, H. Mohamed, B. Myers, L. Dobossy, K. Beyries, D. P. Trosan, F. C. Krebs, V. Miller, K. Stapelmann, *Appl. Sci.* **2020**, *10*(*6*), 2025.
[29] J.W. Lackmann, K. Wende, C. Verlackt, J. Golda, J. Volzke, F. Kogelheide, J. Held, S. Bekeschus, A. Bogaerts, V. Schulz-von der Gathen, K. Stapelmann, *Sci. Rep.* **2018**, *8*(*1*), 7736.
[30] E. Sardella, V. Veronico, R. Gristina, L. Grossi, S. Cosmai, M. Striccoli, M. Buttiglione, F. Fracassi, P. Favia, *Antioxidants* **2021**, *10*(*4*), 605.
[31] P. J. Bruggeman, M. J. Kushner, B. R. Locke, J. G. E. Gardeniers, W. G. Graham, D. B. Graves, R. C. H. M. Hofman-Caris, D. Maric, J. P. Reid, E. Ceriani, D. Fernandez Rivas, J. E. Foster, S. C. Garrick, Y. Gorbanev, S. Hamaguchi, F. Iza, H. Jablonowski, E. Klimova, J. Kolb, F. Krcma, P. Lukes, Z. Machala, I. Marinov, D. Mariotti, S. Mededovic Thagard, D. Minakata, E. C. Neyts, J. Pawlat, Z. Lj Petrovic, R. Pflieger, S. Reuter, D. C. Schram, S. Schroter, M. Shiraiwa, B. Tarabovà, P. A. Tsai, J. R. R. Verlet, T. von Woedtke, K. R. Wilson, K. Yasui, G. Zvereva, *Plasma Sources Sci. Technol.* **2016**, *25*(*5*), 053002.
[32] A. Khlyustova, C. Labay, Z. Machala, M. P. Ginebra, C. Canal, *Chem. Sci. Eng* **2019**, *13*(*2*), 238.
[33] F. Girard-Sahun, V. Badets, P. Lefrançois, N. Sojic, F. Clement, S. Arbault, *Anal. Chem.* **2019**, *91*(*13*), 8002.
[34] V. Gamaleev, N. Iwata, M. Hori, M. Hiramatsu, M. Ito, *Appl. Sci.* **2019**, *9*(*17*), 3505.
[35] Z. Liu, C. Zhou, D. Liu, T. He, L. Guo, D. Xu, M. G. Kong, *AIP Adv.* **2019**, *9*(*1*), 015014.
[36] T. R. Brubaker, K. Ishikawa, K. Takeda, J. Oh, H. Kondo, H. Hashizume, H. Tanaka, S. D. Knecht, S. G. Bilén, M. Hori, *J. Appl. Phys.* **2017**, *122*(*21*), 213301.
[37] B. He, y Ma, X. Gong, Z. Long, J. Li, Q. Xiong, H. Liu, Q. Chen, X. Zhang, S. Yang, Q. H. Liu, *J. Phys. Appl. Phys.* **2017**, *50*(*44*), 445207.
[38] H. Tresp, M. U. Hammer, J. Winter, K.D. Weltmann, S. Reuter, *J. Phys. Appl. Phys.* **2013**, *46*(*43*), 435401.
[39] S. Ikawa, A. Tani, Y. Nakashima, K. Kitano, *J. Phys. Appl. Phys* **2016**, *49*(*42*), 425401.
[40] J. Chauvin, F. Judée, M. Yousfi, P. Vicendo, N. Merbahi, *Sci. Rep.* **2017**, *7*(*1*), 4562.
[41] A. Lin, Y. Gorbanev, J. de Backer, J. van Loenhout, W. van Boxem, F. Lemière, P. Cos, E. Smits, A. Bogaerts, *Adv. Sci.* **2019**, *6*(*6*), 18020626.
[42] A. Gomes, E. Fernandes, J. L. F. C. Lima, *J. Biochem. Biophys. Methods* **2005**, *65*(*2–3*), 45.
[43] B. Tarabová, P. Lukeš, M. U. Hammer, H. Jablonowski, T. von Woedtke, S. Reuter, Z. Machala, *Phys. Chem. Chem. Phys.* **2019**, *21*(*17*), 8883.
[44] E. S. Massima Mouele, O. Ojo Fatoba, O. Babajide, K. O. Badmus, L. F. Petrik, *Environ. Sci. Pollut. Res.* **2018**, *25*(*10*), 9265.
[45] Z. Nasri, G. Bruno, S. Bekeschus, K.-D. Weltmann, T. von Woedtke, K. Wende, *Sens. Actuators B. Chem.* **2021**, *326*, 129007.
[46] G. Bartosz, *Clin. Chim. Acta* **2006**, *368*(*1–2*), 53.
[47] I. Trizio, E. Sardella, V. Rizzi, G. Dilecce, P. Cosma, M. Schmidt, T. von Woedtke, R. Gristina, P. Favia, *Plasma Med.* **2016**, *6*(*1*), 13.
[48] I. Trizio, E. Sardella, E. Francioso, G. Dilecce, V. Rizzi, P. Cosma, M. Schmidt, M. Hänschd, T. von Woedtke, P. Favia, R. Gristina, *Clin. Plasma Med.* **2015**, *3*(*2*), 62.
[49] K. Wende, P. Williams, J. Dalluge, W. van Gaens, H. Aboubakr, J. Bischof, T. von Woedtke, S. M. Goyal, K. Wetlmann, A. Bogaerts, K. Masur, P. J. Bruggeman, *Biointerphases* **2015**, *10*(*2*), 029518.
[50] P. Heirman, W. van Boxem, A. Bogaerts, *Phys. Chem. Chem. Phys.* **2019**, *21*(*24*), 12881.
[51] P.-M. Girard, A. Arbabian, M. Fleury, G. Bauville, V. Puech, M. Dutreix, J. Santos, *Sci. Rep.* **2016**, *6*(*1*), 29098.
[52] C. E. Anderson, N. R. Cha, A. D. Lindsay, D. S. Clark, D. B. Graves, *Plasma Chem. Plasma Process.* **2016**, *36*(*6*), 1393.
[53] C. N. Satterfield, A. H. Bonnell, *Anal. Chem.* **1955**, *27*(*7*), 1174.
[54] G. Eisenberg, *Ind. Eng. Chem., Anal. Ed.* **1943**, *15*(*5*), 327.
[55] T. von Woedtke, T. Oehmigen, K. Brandenburg, R. Hoder, T. Wilke, C. Hähnel, M. Weltmann, in *Plasma for Bio-Decontamination, Medicine and Food Security*, Springer, Dordrecht, The Netherlands **2012**, p. 67.
[56] M. Anbar, H. Taube, *J. Am. Chem. Soc.* **1954**, *76*(*24*), 6243.
[57] E. Pick, Y. Keisari, *J. Immunol. Methods* **1980**, *38*(*1–2*), 161.
[58] N. Nguyen, H. Park, S. Hwang, J.-S. Lee, S. Yang, *Appl. Sci.* **2019**, *9*(*4*), 801.
[59] D. Dębski, R. Smulik, J. Zielonka, B. Michałowski, M. Jakubowska, K. Dębowska, J. Adamus, A. Marcinek,

B. Kalyanaraman, A. Sikora, *Free Radicals Biol. Med.* **2016**, *95*, 323.
[60] Y. F. Yue, S. Mohades, M. Laroussi, X. Lu, *IEEE Trans. Plasma Sci.* **2016**, *44*(*11*), 2754.
[61] T. W. Chen, C. Liu, C. Chen, M. Wu, P. Chien, Y. Cheng, J. Wu, *ECS J. Solid State Sci. Technol.* **2020**, *9*(*11*), 115002.
[62] M. Mateu-Sanz, J. Tornìn, B. Brulin, A. Khlyustova, M. P. Ginebra, P. Layrolle, C. Canal, *Cancers* **2020**, *12*(*1*), 227.
[63] H. Tresp, M. U. Hammer, K.-D. Weltmann, S. Reuter, *Plasma Med.* **2013**, *3*(*1–2*), 45.
[64] D. Yan, H. Cui, W. Zhu, A. Talbot, L. G. Zhang, J. H. Sherman, M. Keidar, *Sci. Rep.* **2017**, *7*(*1*), 1.
[65] C. Gay, J. Collins, J. M. Gebicki, *Anal. Biochem.* **1999**, *273*(*2*), 149.
[66] M. Gülden, A. Jess, J. Kammann, E. Maser, H. Seibert, *Free Radic. Biol. Med.* **2010**, *49*(*8*), 1298.
[67] K. Kosaka, H. Yamada, S. Matsui, S. Echigo, K. Shishida, *Environ. Sci. Technol.* **1998**, *32*(*23*), 3821.
[68] G. R. A. Johnson, N. B. Nazhat, *J. Am. Chem. Soc.* **1987**, *109*(*7*), 1990.
[69] K. V. Ponganis, M. A. de Araujo, H. L. Hodges, *Inorg. Chem.* **1980**, *19*(*9*), 2704.
[70] G. Davies, R. Higgins, D. J. Loose, *Inorg. Chem.* **1976**, *15*(*3*), 700.
[71] S. Goldstein, G. Czapski, *J. Free Radicals Biol. Med.* **1985**, *1*(*5–6*), 373.
[72] A. N. Baga, G. R. A. Johnson, N. B. Nazhat, R. A. Saadalla-Nazhat, *Anal. Chim. Acta* **1988**, *204*, 349.
[73] T. M. Florence, J. L. Stauber, K. J. Mann, *J. Inorg. Biochem.* **1985**, *24*(*4*), 243.
[74] I. Guevara, J. Iwanejko, A. Dembińska-Kieć, J. Pankiewicz, A. Wanat, P. Anna, I. Gołabek, S. Bartuś, M. Malczewska-Malec, A. Szczudlik, *Clin. Chim. Acta* **1998**, *274*(*2*), 177.
[75] Q. H. Wang, L. Yu, Y. Liu, L. Lin, R. Lu, J. Zhu, L. He, Z. Lu, *Talanta* **2017**, *165*, 709.
[76] D. Giustarini, R. Rossi, A. Milzani, I. Dalle-Donne, in *Methods in Enzymology*, 440, Elsevier, Waltham, MA **2008**.
[77] K. M. Miranda, M. G. Espey, D. A. Wink, *Nitric Oxide* **2001**, *5*(*1*), 62.
[78] A. M. Hartley, R. I. Asai, *Anal. Chem.* **1963**, *35*(*9*), 1207.
[79] D. W. W. Andrews, *Analyst* **1964**, *89*(*1064*), 730.
[80] N. Raikos, K. Fytianos, C. Samara, V. Samanidou, *Für Anal. Chem.* **1998**, *331*(*5*), 495.
[81] A. M. Hartley, R. I. Asai, *J. Am. Water Works Assoc.* **1960**, *52*(*2*), 255.
[82] L. Bulgariu, D. Bulgariu, *Rev. Anal. Chem.* **2012**, *31*(*3–4*), 201.
[83] H. A. C. Montgomery, J. F. Dymock, *Analyst* **1962**, *87*(*1034*), 374.
[84] R. Michalski, I. Kurzyca, *Pol. J. Environ. Stud.* **2006**, *15*(*1*), 5.
[85] J. B. Harborne, in *Phytochemical Methods*, Springer, Dordrecht, The Netherlands **1973**, p. 33.

How to cite this article: V. Veronico, P. Favia, F. Fracassi, R. Gristina, E. Sardella.Validation of colorimetric assays for hydrogen peroxide, nitrate and nitrite ions in complex plasma-treated water solutions. *Plasma Processes Polym*. 2021;e2100062. https://doi.org/10.1002/ppap.202100062